Progress In Electromagnetics Research, PIER 97, 27–43, 2009

PERMITTIVITY DETERMINATION OF FRESH CEMENT-BASED MATERIALS BY AN OPEN-ENDED WAVEGUIDE PROBE USING AMPLITUDE-ONLY MEASUREMENTS

U. C. Hasar †

Department of Electrical and Electronics Engineering
Ataturk University
Erzurum 25240, Turkey

Abstract—An open-ended waveguide probe has been adapted for complex permittivity determination and hence mechanical property inspection of cement-based materials. The probe uses amplitude-only reflection measurements at different frequencies for this goal, which is suitable for industrial based applications when cost and ease of use are important considerations. We have derived expressions by taking into account of the wave-material interaction. The reference plane for measurements is set inside the waveguide to measure solely the reflected signal of the dominant mode. It is shown that the measurement results are in good agreement with the theory.

1. INTRODUCTION

Material research has provided many dielectric materials for application in industry. With increasing utilization of different materials, including composite materials, there is a growing industrial demand for dielectric characterization of these materials for design, manufacturing, and quality control purposes in industries such as civil, aerospace, electronics, chemical, etc. [1–8]. Many factors such as the frequency range, required measurement accuracy, sample size, state of the material (liquid, solid, powder and so forth), destructiveness and non-destructiveness, contacting and non-contacting, etc. have to be considered when choosing the appropriate technique to obtain the desired information on the dielectric properties [1, 9].

Corresponding author: U. C. Hasar (ugurcem@atauni.edu.tr).
† Also with Department of Electrical and Computer Engineering, Binghamton University, Binghamton 13902, NY, USA.

Resonant methods have much better accuracy and sensitivity than nonresonant ones [1]. They can be applied to characterization of low-loss as well as high-loss materials [1, 10], though, a meticulous sample preparation is needed before measurements. In addition, for an analysis over a broad frequency band, a new measurement set-up (a cavity) must be made. This is not feasible from a practical point of view. Furthermore, these methods generally assume that the sample does not alter the resonant frequency and slightly decrease the quality factor to apply sample perturbation technique [1]. Due to their relative simplicity, nonresonant waveguide transmission/reflection methods are presently the most widely used broadband measurement techniques [11]. These methods have effectively been applied to determine relative complex permittivity (ε_r) of materials [12–16]. However, these methods together with resonant methods are destructive since they require elaborate sample cutting to fit the sample into its holder. Therefore, the solutions to nondestructive ε_r measurements of a material at higher frequencies are limited to open-ended coaxial [17, 18], parallel-plate waveguide [9], open-ended rectangular waveguide [19–23] and free-space methods [24–26].

Free-space methods are contactless and thus suitable for measurements at high-temperatures [1]. However, they suffer from the diffraction at the edges of the sample. In order to reduce this effect, the transverse dimensions (height and width) of the sample can be selected sufficiently large. As another solution, spot focusing horn-lens antennas can be employed [1]. Nonetheless, the bandwidth of this antenna system is limited due to focusing nature of the lens. As a final solution, a calibration procedure which takes into account of the diffraction effects can be incorporated to the measurement system [25, 26]. The accuracy of free-space methods, however, is not so high since the footstep of the propagation is relatively large if the sample is placed at far zone.

Parallel-plate waveguide or parallel-plate transmission lines with multiple modes can be utilized for nondestructive ε_r measurements of materials. Although the accuracy of this approach is very good [9], for practical applications, it is not easy to have parallel-plates with infinite transverse dimensions to eliminate fringing fields at the plate corners. From practical-point of view, open-ended coaxial lines and open-ended waveguides can efficiently be used for ε_r measurements.

The mechanical properties of cement-based materials are needed by designers for stiffness and deflections evaluation and are fundamental properties required for the proper modeling of their constitutive behaviors and for their proper uses in various structural applications. For this reason, determination of mechanical properties

of cement-based composites has become very important from the point of view of design [27, 28]. General methods used in civil engineering for characterizing the mechanical properties of cement-based materials are either to prepare a specimen with the same mix proportions in the lab, or to drill a specimen from the structure, and then test in the lab. The preparation method does not reflect the actual measure of interest since the specimen in the lab and materials cast in the field are not cured same [29]. The removal method is clearly harmful to the overall structure as a result of removing a test sample (removed sample). The test techniques used for both methods are destructive [30] because the sample is damaged and cannot be reused in future. Several non-destructive evaluation (NDE) techniques have been applied to quality assessment, mixture content evaluation, and monitoring the internal integrity (voids, cracks, degradation, etc.) of cement-based materials [31]. These techniques are ultrasound, infrared thermography, radiography, ground-penetrating radar, and microwaves. Compared to other NDE techniques, microwaves are not hazardous, scatter little compared to acoustic waves, are low in cost as compared to radioactive methods, are noncontact (microwave sensor-antenna), and have a good spatial resolution and superior penetration in nonmetallic materials [27].

A close correlation between ε_r measurements and mechanical properties (i.e., compressive strength) of cement-based materials can be established [29]. In addition, ε_r measurements are necessary in propagation-related research especially in predicting the channel properties such as path loss and delay spread in complex environments [32]. In the literature, ε_r measurements of cement-based materials by an open-ended waveguide probe were realized by complex reflection measurements at the waveguide aperture. In this research paper, we will utilize a simple and relatively inexpensive microwave set-up, which is suitable for industrial-based applications, constructed from discrete microwave components for ε_r measurements of fresh cement-based materials by using amplitude-only reflection measurements from an open-ended waveguide probe at different frequencies.

2. MODEL FOR THE PROBLEM

2.1. Field Expressions

The problem investigated is depicted in Fig. 1. In this figure, an open-ended waveguide covered with a low-loss sample with thickness L is terminated in a high-loss cement sample. We utilize the low-loss sample so as to prevent water-like cement-sample from seeping into waveguide

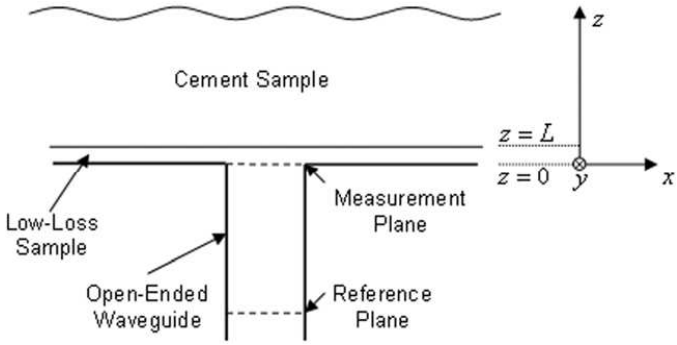

Figure 1. Measurement configuration for permittivity determination of fresh cement-based samples by an open-end waveguide probe (open-ended waveguide with a low-loss sample).

and have a flat plane at $z = L$. The waveguide aperture is located in the xy plane and positioned at $z = 0$. It is assumed that waveguide flanges, transverse dimensions of the low-loss sample and cement-sample extend to infinity in both x and y directions. It is noted that, by assuming that waveguide flanges are perfect electric conductors (PECs) and extend to infinity, and the cement-sample is lossy (which is a real condition for fresh cement samples), the derived electric and magnetic field expressions in the unbounded regions (outside of the aperture) can be uniquely specified by the aperture sources and tangential field components over a PEC [33].

In the following theoretical investigation, a harmonic time variation of the type $e^{j\omega t}$ is used, and we assume that waveguide walls and flanges are PECs. For the expressions of the fields inside the waveguide, electric and magnetic vector potentials (or Hertzian vectors), $\vec{A}$ and $\vec{F}$, can be utilized [33]. Assuming that the waveguide operates at its dominant mode (TE^z_{10}), and the low-loss sample has a flat surface, vector potentials for incident and reflected fields can be written as

$$\vec{F}^i(x,y,z) = \vec{a}_z A_{10} \cos(\beta_{x1} x)\, e^{-j\beta_{z10} z} \tag{1}$$

$$\vec{F}^r(x,y,z) = \vec{a}_z \sum_{\substack{m,n=0 \\ m=n\neq 0}}^{\infty} C_{mn} \cos(\beta_{xm} x) \cos(\beta_{yn} y)\, e^{j\beta_{zmn} z} \tag{2}$$

where

$$\beta_{xm} = \frac{m\pi}{a},\ \beta_{yn} = \frac{n\pi}{b},\ \beta_{zmn} = \sqrt{\beta^2 - \beta^2_{xm} - \beta^2_{yn}},\ \beta = \frac{\omega}{c}. \tag{3}$$

In (1)–(3), the superscripts 'i' and 'r', respectively, signify the incident

and reflected fields; A_{10} and C_{mn} are the amplitudes (unknown) of the vectors; a and b are the broad and narrow dimensions of the waveguide aperture; m and n, respectively, denote how many one-half apparent wavelengths in x and y directions inside the waveguide cross section; β_{x_m}, β_{y_n} and $\beta_{z_{mn}}$ are, respectively, the apparent phase constants (or wavenumbers) in x, y and z directions; ω is the angular frequency; c is the velocity of light in vacuum.

For a complete solution, both TE^z and TM^z modes should be considered inside and outside the waveguide. For simplicity, we restrict the analysis to only TE modes. The reasoning for this will be discussed later. Then, for a source-free waveguide aperture region, using the following expressions [33]

$$\vec{E}^{i,r} = -j\left\{\omega\vec{A}^{i,r} - \frac{1}{\omega\mu_0\varepsilon_0}\nabla\left(\nabla\cdot\vec{A}^{i,r}\right)\right\} - \frac{1}{\varepsilon_0}\nabla\times\vec{F}^{i,r},\ \vec{A}^{i,r} = 0 \quad (4)$$

$$\vec{H}^{i,r} = -j\left\{\omega\vec{F}^{i,r} + \frac{1}{\omega\mu_0\varepsilon_0}\nabla\left(\nabla\cdot\vec{F}^{i,r}\right)\right\} + \frac{1}{\mu_0}\nabla\times\vec{A}^{i,r},\ \vec{A}^{i,r} = 0, \quad (5)$$

the incident and reflected electric and magnetic fields can be derived from (1) and (2) as

$$E_y^i(x,z) = -A_{10}\frac{\beta_{x1}}{\varepsilon_0}\sin(\beta_{x1}x)\,e^{-j\beta_{z10}z}, \quad (6)$$

$$H_x^i(x,z) = A_{10}\frac{\beta_{x1}\beta_{z10}}{\omega\mu_0\varepsilon_0}\sin(\beta_{x1}x)\,e^{-j\beta_{z10}z}, \quad (7)$$

$$H_z^i(x,z) = -jA_{10}\frac{\beta_d^2-\beta_{z10}^2}{\omega\mu_0\varepsilon_0}\cos(\beta_{x1}x)\,e^{-j\beta_{z10}z}, \quad (8)$$

$$E_x^r(x,y,z) = C_{mn}\frac{\beta_{yn}}{\varepsilon_0\varepsilon_{rd}}\cos(\beta_{xm}x)\sin(\beta_{yn}y)\,e^{-j\beta_{zmn}z}, \quad (9)$$

$$E_y^r(x,y,z) = -C_{mn}\frac{\beta_{xm}}{\varepsilon_0\varepsilon_{rd}}\sin(\beta_{xm}x)\cos(\beta_{yn}y)\,e^{-j\beta_{zmn}z}, \quad (10)$$

$$H_x^r(x,y,z) = C_{mn}\frac{\beta_{xm}\beta_{zmn}}{\omega\mu_0\varepsilon_0\varepsilon_{rd}}\sin(\beta_{xm}x)\cos(\beta_{yn}y)\,e^{-j\beta_{zmn}z}, \quad (11)$$

$$H_y^r(x,y,z) = C_{mn}\frac{\beta_{yn}\beta_{zmn}}{\omega\mu_0\varepsilon_0\varepsilon_{rd}}\cos(\beta_{xm}x)\sin(\beta_{yn}y)\,e^{-j\beta_{zmn}z}, \quad (12)$$

$$H_z^r(x,y,z) = -jC_{mn}\frac{\beta_d^2-\beta_{zmn}^2}{\omega\mu_0\varepsilon_0\varepsilon_{rd}}\cos(\beta_{xm}x)\cos(\beta_{yn}y)e^{-j\beta_{zmn}z}. \quad (13)$$

It is obvious that, for a section of waveguide where there are no actual sources, the electric and magnetic field expressions corresponding to different modes in (6)–(13) satisfy Lorenz reciprocity condition, which in turn validates them [33].

Assuming uniform unbounded regions outside waveguide aperture, the basic procedure for obtaining the expressions for transmitted fields in these regions is to use Fourier integral pairs to map spatial dependencies of electric and magnetic fields into spatial periods [19–23]. It is well known that electric and magnetic fields have spatial periods which are functions of the aperture. Since the electric and magnetic fields have some non-zero values over the aperture and zero values elsewhere (a consequence of the assumption of PEC), we can utilize Fourier integral pairs for these fields over the aperture. As a result, the problem under investigation (2-D problem) is transferred from the spatial analysis into the determination of Fourier integral pairs, given as [34]

$$f(x,y,z) = \frac{1}{4\pi^2}\int_{-\infty}^{\infty}\int_{-\infty}^{\infty}\tilde{f}(k_x,k_y,z)\,e^{jk_x x}e^{jk_y y}dk_x dk_y, \tag{14}$$

$$\tilde{f}(k_x,k_y,z) = \int_{-\infty}^{\infty}\int_{-\infty}^{\infty}f(x,y,z)\,e^{-jk_x x}e^{-jk_y y}dxdy, \tag{15}$$

where k_x and k_y denote spatial wavenumbers in x and y dimensions, and $f(x,y,z)$ and $\widetilde{f}(k_x,k_y,z)$ represent the basis of the angular spectrum method. It should be stressed that, to apply the Fourier integral pairs to our problem, the function $f(x,y,z)$ (a representative for the components of electric and magnetic fields) must be continuous or have only a finite number of finite discontinuities in any finite interval and must be absolutely integrable [34], that is

$$\int_{-\infty}^{\infty}\int_{-\infty}^{\infty}\left|f(x,y,z)\,e^{-jk_x x}e^{-jk_y y}\right|dxdy = \int_{-\infty}^{\infty}\int_{-\infty}^{\infty}|f(x,y,z)|\,dxdy < \infty. \tag{16}$$

The vector potentials for each region in Fig. 1 (low-loss sample and lossy cement-sample) expressed by (14) must satisfy the source-free vector wave equation which is reduced to

$$\frac{d^2\tilde{F}_z^{tl}(k_x,k_y,z)}{dz^2} - \gamma_l^2\tilde{F}_z^{tl}(k_x,k_y,z) = 0,$$
$$\gamma_l = \sqrt{k_x^2+k_y^2-\beta_l^2},\ l=1,2, \tag{17}$$

where γ_l and β_l are the propagation factor and phase constant in region l; l indicates each unbounded region in Fig. 1; the superscript 't' denotes the transmitted fields. The solution of (17) can be written as

$$\tilde{F}_z^{tl}(k_x,k_y,z) = \tilde{F}_{zl}^{+}(k_x,k_y)\,e^{-\gamma_l z} + \tilde{F}_{zl}^{-}(k_x,k_y)\,e^{\gamma_l z}, \tag{18}$$

where $\mathrm{Re}\{\gamma_l\} \geq 0$ and $\mathrm{Im}\{\gamma_l\} \geq 0$ [21, 23] for a meaningful attenuation and phase constant quantities in z and $-z$ directions and $\tilde{F}_{zl}^{+}(k_x, k_y)$ and $\tilde{F}_{zl}^{-}(k_x, k_y)$ are the forward and backward travelling vector amplitudes to be determined by application of boundary conditions. As a result, electric and magnetic field expressions for unbounded regions can be found using (4), (5), (14).

2.2. Boundary Conditions and Derivation of Reflection Coefficient

Using (14) and (18), transmitted electric and magnetic fields in each unbounded region can be written as

$$E_y^{t^l}(x,y,z) = \frac{1}{4\pi^2}\int_{-\infty}^{\infty}\int_{-\infty}^{\infty}\left[\tilde{E}_{yl}^{+}(k_x,k_y)\,e^{-\gamma_l z} + \tilde{E}_{yl}^{-}(k_x,k_y)\,e^{\gamma_l z}\right]e^{jk_x x}e^{jk_y y}dk_x dk_y, \quad (19)$$

$$H_x^{t^l}(x,y,z) = \frac{1}{4\pi^2}\int_{-\infty}^{\infty}\int_{-\infty}^{\infty}\frac{\left[-\gamma_l\tilde{E}_{yl}^{+}(k_x,k_y)e^{-\gamma_l z}+\gamma_l\tilde{E}_{yl}^{-}(k_x,k_y)e^{\gamma_l z}\right]}{j\omega\mu_0}e^{jk_x x}e^{jk_y y}dk_x dk_y \quad (20)$$

where, for derivation of (20), we applied $(\nabla \times \vec{E})_x = -j\omega\mu_0 H_x$ using (19). Since electric and magnetic fields in (19) and (20) for each unbounded region must satisfy the source-free vector wave equation, their angular spectrum terms will be in a similar form as $\widetilde{F}_z^{tl}(k_x, k_y, z)$ in (18).

In each unbounded region, both forward and backward traveling wave amplitudes should generally exist. We apply the following boundary conditions to any value of k_x, k_y, x and y as

$$\begin{aligned} &E_y^{t^2}(x,y,z=\infty) \to 0,\ H_x^{t^2}(x,y,z=\infty) \to 0 \\ &E_y^{t^2}(x,y,z=L) = E_y^{t^1}(x,y,z=L), \\ &H_x^{t^2}(x,y,z=L) = H_x^{t^1}(x,y,z=L). \end{aligned} \quad (21)$$

The first condition in (21) results from the application of radiation boundary condition, which is essentially a statement of energy conversation; at an infinite distance from a finite-valued source, the fields must be vanishingly small (i.e., zero) [33]. In addition, according to the uniqueness theorem, for the fields in unbounded regions to be uniquely specified, this condition should be met [33]. The first boundary condition in (21) is valid for a lossy medium and not directly

applicable to free-space. To justify this condition (or somehow the uniqueness theorem for a lossless medium), the fields in a lossless medium can be considered to be the limit of the corresponding fields in a lossy medium as the dissipation approaches zero [33].

Using the remaining boundary conditions in (21), we derive a term which will be used for the derivation of the reflection coefficient at the aperture as

$$\alpha_1(k_x,k_y)=\tilde{E}_{y1}^{-}(k_x,k_y)/\tilde{E}_{y1}^{+}(k_x,k_y)=(\gamma_1-\gamma_2)\,e^{-2\gamma_1 L}/(\gamma_1+\gamma_2)\,. \tag{22}$$

At the waveguide aperture, we use the following boundary conditions

$$E_y^{t^1}(0\le x\le a,\,0\le y\le b,\,z=0)= E_y^{i}(0\le x\le a,\,z=0)+E_y^{r}(0\le x\le a,\,0\le y\le b,\,z=0)\,, \tag{23}$$

$$H_x^{t^1}(0\le x\le a,\,0\le y\le b,\,z=0)= H_x^{i}(0\le x\le a,\,z=0)+H_x^{r}(0\le x\le a,\,0\le y\le b,\,z=0)\,. \tag{24}$$

Application of the boundary condition in (23) yields

$$\tilde{E}_{y1}^{+}(k_x,k_y)= \frac{\left[-\frac{\beta_{x1}A_{10}}{\varepsilon_0}S_1(k_x)\,C_0(k_y)-\sum\limits_{\substack{m,n=0\\ m=n\neq 0}}^{\infty}\frac{C_{mn}\beta_{xm}}{\varepsilon_0}S_m(k_x)C_n(k_y)\right]}{(1+\alpha_1(k_x,k_y))}, \tag{25}$$

where $\alpha_1(k_x,k_y)$ is given in (22) and

$$S_m(k_x)=\int_0^a \sin(\beta_{xm}x)e^{-jk_x x}dx=\frac{\beta_{xm}}{(k_x^2-\beta_{xm}^2)}\left((-1)^m e^{-jk_x a}-1\right), \tag{26}$$

$$C_n(k_y)=\int_0^b \cos(\beta_{yn}y)e^{-jk_y y}dy=\frac{jk_y}{\left(k_y^2-\beta_{yn}^2\right)}\left((-1)^n e^{-jk_y b}-1\right). \tag{27}$$

Integrals in (26) and (27) are extended to the aperture of the rectangular waveguide using the expression in (15).

In a similar fashion, applying the boundary condition in (24), we

find

$$A_{10}\frac{\beta_{x1}\beta_{z10}}{\omega\mu_0\varepsilon_0}\sin(\beta_{x1}x)+\sum_{\substack{m,n=0\\m=n\neq 0}}^{\infty}C_{mn}\frac{\beta_{xm}\beta_{zmn}}{\omega\mu_0\varepsilon_0}\sin(\beta_{xm}x)\cos(\beta_{yn}y)$$

$$=-\frac{1}{4\pi^2}\int_{-\infty}^{\infty}\int_{-\infty}^{\infty}\frac{\gamma_1}{j\omega\mu_0}\tilde{E}_{y1}^{+}(k_x,k_y)\left(1-\alpha_1(k_x,k_y)\right)e^{jk_xx}e^{jk_yy}dk_xdk_y. \quad (28)$$

Substituting $\tilde{E}_{y1}^{+}(k_x,k_y)$ of (25) into (28), we obtain

$$A_{10}\frac{\beta_{x1}\beta_{z10}}{\omega\mu_0\varepsilon_0}\sin(\beta_{x1}x)+\sum_{\substack{m,n=0\\m=n\neq 0}}^{\infty}C_{mn}\frac{\beta_{xm}\beta_{zmn}}{\omega\mu_0\varepsilon_0}\sin(\beta_{xm}x)\cos(\beta_{yn}y)$$

$$=-\frac{1}{4\pi^2}\int_{-\infty}^{\infty}\int_{-\infty}^{\infty}\left[-\frac{\beta_{x1}A_{10}}{\varepsilon_0}S_1(k_x)C_0(k_y)-\sum_{\substack{m,n=0\\m=n\neq 0}}^{\infty}\frac{C_{mn}\beta_{xm}}{\varepsilon_0}S_m(k_x)C_n(k_y)\right]$$

$$\times\frac{\gamma_1}{j\omega\mu_0}G(k_x,k_y)\,e^{jk_xx}e^{jk_yy}dk_xdk_y. \quad (29)$$

where

$$G(k_x,k_y)=\left(1-\alpha_1(k_x,k_y)\right)/\left(1+\alpha_1(k_x,k_y)\right). \quad (30)$$

In order to use the orthogonality property of the field expressions [33], we multiply (29) with $\sin(\beta_{xp}x)\cos(\beta_{yq}y)$ and integrate over the waveguide aperture. After arranging, we obtain

$$\frac{ab}{2}\delta_{0q}\delta_{p1}+\frac{ab}{4}\sum_{p=1}^{\infty}\sum_{q=0}^{\infty}C_{pq}\frac{\beta_{xp}\beta_{zpq}}{\omega\mu_0\varepsilon_0}\left(2\delta_{0q}+\delta_{pq}\right)$$

$$=-j\frac{\gamma_1}{\omega\mu_0\varepsilon_0}\left\{A_{10}\beta_{x1}J_{10pq}+\sum_{\substack{m,n=0\\m=n\neq 0}}^{\infty}C_{mn}\beta_{xm}J_{mnpq}\right\}, \quad (31)$$

where

$$\delta_{pq}=\begin{cases}1 & \text{if } p=q\\ 0 & \text{otherwise}\end{cases} \quad (32)$$

$$J_{mnpq}=\frac{1}{4\pi^2}\int_{-\infty}^{\infty}\int_{-\infty}^{\infty}G(k_x,k_y)S_m(k_x)C_n(k_y)S_p(-k_x)C_q(-k_y)\,dk_xdk_y. \quad (33)$$

For the evaluation of J_{mnpq} in (33), one can apply the Parseval's theorem, separate the integrand into two separate functions and finally take their respective inverse Fourier transforms [21]. For more details, the reader can refer to [34].

3. PERMITTIVITY DETERMINATION

After solving the unknown coefficients C_{mn} in (31), the reflection coefficient at the aperture of the probe S_{11}^{m} (or measurement plane) can be found by

$$S_{11}^{m}(\omega) = C_{mn}/A_{10}. \tag{34}$$

It is noted that, in addition to the reflected fields of TE^z, TM^z fields will appear at the waveguide aperture if one considers magnetic field vector potential in unbounded regions. However, assuming that the reference plane is at least two times free-space wavelength away from the measurement plane, the effect of reflected fields with all TM^z modes together with all TE^z modes except the one with an amplitude of C_{10} can be neglected [11, 13–16]. Therefore, the assumption that an analysis based on only TE_{mn}^{z} modes is sufficient for our problem is practically valid. Then, the reflection coefficient at the reference plane can be written as

$$S_{11}^{r}(\omega) = C_{10}/A_{10}. \tag{35}$$

Since the reflection coefficient is frequency dependent, amplitude-only measurements of $S_{11}^{r}(\omega)$ in (35) at two different frequencies can be utilized for ε_{r_2} determination [35].

4. MEASUREMENTS

The set-up for validating the proposed method is shown in Fig. 2. The source (OSC) operating between 8.2 and 12.5 GHz feeds the measurement system. The signal from the source is modulated by a 1 kHz signal to measure amplitude-modulated reflected signals by a reflectometer constructed from square-law detectors and couplers. While the Coupler I measures incident waves, the Coupler II detects reflection properties. A rotary attenuator (ATT) is used not only for preventing the source from harmful reflections but also for varying the level of the incident signal, which allows us to radiate the same level of incident signal, which is used in the calibration process to send the same level of incident signal.

We performed a simple calibration procedure for relative measurements as follows [36]. Firstly, we positioned a waveguide short at the reference plane (Fig. 1) and then measured amplitude of reflected

signals by the Coupler II. Next, we located the sample on a thin fused quartz sample (5 mm) and re-measured the reflected signals by the Coupler II. During these measurements, we used the same incident signals measured by the Coupler I. Finally, we measured $S_{11}^r(\omega)$ at the reference plane as

$$S_{11}^r(\omega)_{meas} = \sqrt{V_{sr}/V_m} \tag{36}$$

where V_{sr} and V_m are, respectively, the dc voltage values of reflected signals of the sample and metal plate (reference). We connected an extra waveguide section with a length greater than $2c/f$ at X-band between the reference plane and open-ended waveguide aperture to filter out any higher order modes [11].

Since the proposed method relies on the computation of C_{10} using C_{mn} in (31), and there are infinite sets of linear equations in (31), the computations should be performed with a finite set of equations. It is assumed that the final convergence to the solution of $S_{11}^r(\omega)$ is obtained by considering twenty modes [9, 21]. We noted that eight modes are sufficient to obtain highly accurate results. Because the proposed method exploits amplitude-only measurements at different frequencies for permittivity determination, permittivity of materials can be determined using two approaches: namely, frequency-independent or frequency-dependent [37]. While the former assumes that permittivity slightly changes with frequency, the latter takes into account of a change in permittivity with frequency. Since high-loss samples are more frequency-dependent than low-loss samples, the latter approach is more suitable. Using this approach, permittivity can be modeled as a function of finite power series [35, 37]. Selection of the degree of approximation by power series depends on the frequency behavior of the sample. For selection of the appropriate frequencies for the permittivity determination, in this paper, we apply the simple approach adopted in [37]. For more details, reader can refer to [37].

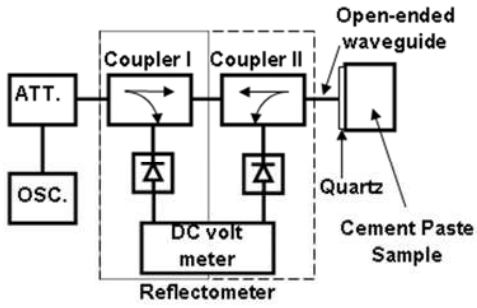

Figure 2. Measurement set-up for validation of the proposed method.

For validation of the method, we prepared some fresh cement samples with different water-to-cement ratios (w/c). Then, we poured them into a plastic container whose transverse dimensions are approximately 30 cm × 30 cm × 15 cm. Next, we pointed the probe (open-ended waveguide with thin quartz sample) onto the prepared samples. Finally, we measured the permittivity by the proposed method. For example, Figs. 3 and 4 demonstrate the measured complex permittivity of two cement paste specimens (a mixture of water and cement) with different w/c ratios. Both of them were 2-hours aircured at room temperature.

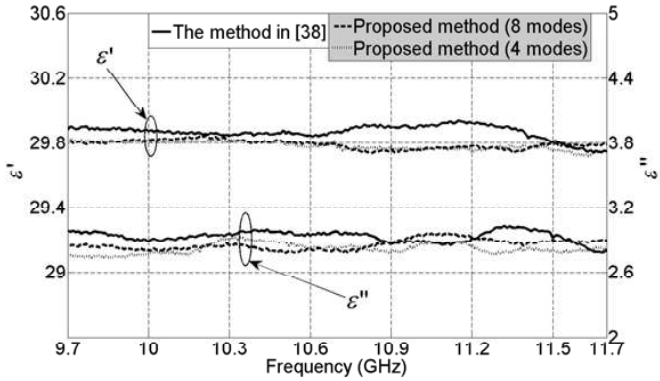

Figure 3. Measured complex permittivity of the prepared cement paste with $w/c = 0.4$.

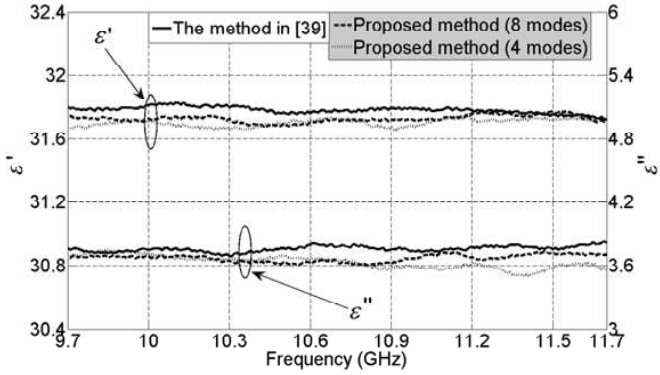

Figure 4. Measured complex permittivity of the prepared cement paste with $w/c = 0.45$.

For verification of the measurements by the proposed method, we also applied two other methods [38, 39]. In the application of these methods, we positioned some of the prepared samples (each 15 mm in length) between two low-loss polytetrafluoro-ethylene (PTFE) samples with different lengths (5 mm and 7 mm) for the method in [38] and identical lengths (5 mm) for the method in [39]. We assumed that the complex permittivities of the quartz and PTFE samples, respectively, are $3.78 - j0.00006$ [40] and $2.043 - j0.00076$ [40, 41]. For calibration of these methods, the thru-reflect-line calibration technique [42] is utilized. We used a waveguide short and the shortest waveguide spacer ($44.38 \mp 5\%$ mm) in our lab for reflection and line standards, respectively. The line has a $\pm 70^\circ$ maximum offset from 90° over 9.7–11.7 GHz.

It is seen from Figs. 3 and 4 that there is a good agreement between measurement results of the proposed method and those of the methods in [38] and [39]. This validates the accuracy and derivations of permittivity in Section 2. The oscillatory behavior of measured permittivity by the method in [38] may arise from the fact that while reflection measurements give information of surface characteristics, transmission measurements show the information of internal structure.

Although the proposed method is applicable in industrial settings, it assumes that the sample under test is homogeneous. In practical applications, a perfect homogeneity in samples is not possible. In these circumstances, a surface scanning of the sample is needed to be sure if the sample is homogeneous or the measurements are accurate. The proposed method may not be so applicable to these applications since it may require considerable amount of time and effort for a complete surface scan of samples with larger transverse dimensions. In such applications, open-ended horn antenna probe seems promising since it combines the better features of free-space measurements (fast surface scanning) and open-ended waveguide measurements (good spatial resolution and accuracy). As a future study, we would like to apply the open-ended horn antenna probe as a means of fast and accurate surface scanning for monitoring the mechanical property inspection of civil structures (buildings, bridges, etc.).

5. CONCLUSION

A feasible waveguide probe has been proposed for permittivity determination of lossy fresh cement-based materials. We have derived expressions for permittivity determination by using amplitude-only reflection measurements. The proposed method is validated by permittivity measurements of prepared cement paste samples.

ACKNOWLEDGMENT

U. C. Hasar (Mehmetcik) would like to thank TUBITAK (The Scientific and Technological Research Council of Turkey) Münir Birsel National Doctorate Scholarship, YOK (The Higher Education Council of Turkey) Doctorate Scholarship, the Leopold B. Felsen Fund with an outstanding young scientist award in electromagnetics for supporting his studies.

REFERENCES

1. Chen, L. F., C. K. Ong, C. P. Neo, et al., *Microwave Electronics: Measurement and Materials Characterization*, John Wiley & Sons, West Sussex, England, 2004.
2. He, X., Z. X. Tang, B. Zhang, and Y. Wu, "A new deembedding method in permittivity measurement of ferroelectric thin film material," *Progress In Electromagnetics Research Letters*, Vol. 3, 1–8, 2008.
3. Wu, Y. Q., Z. X. Tang, Y. H. Xu, X. He, and B. Zhang, "Permittivity measurement of ferroelectric thin film based on CPW transmission line," *Journal of Electromagnetic Waves and Applications*, Vol. 22, No. 4, 555–562, 2008.
4. Zainud-Deen, S. H., M. E. S. Badr, E. El-Deen, and K. H. Awadalla, "Microstrip antenna with corrugated ground plane structure as a sensor for landmines detection," *Progress In Electromagnetics Research B*, Vol. 2, 259–278, 2008.
5. Zainud-Deen, S. H., W. M. Hassen, E. El deen Ali, and K. H. Awadalla, "Breast cancer detection using a hybrid finite difference frequency domain and particle swarm optimization techniques," *Progress In Electromagnetics Research B*, Vol. 3, 35–46, 2008.
6. Yan, L. P., K. M. Huang, and C. J. Liu, "A noninvasive method for determining dielectric properties of layered tissues on human back," *Journal of Electromagnetic Waves and Applications*, Vol. 21, No. 13, 1829–1843, 2007.
7. Zainud-Deen, S. H., M. E. S. Badr, E. El-Deen, K. H. Awadalla, and H. A. Sharshar, "Microstrip antenna with defected ground plane structure as a sensor for landmines detection," *Progress In Electromagnetics Research B*, Vol. 4, 27–39, 2008.
8. Capineri, L., D. J. Daniels, P. Falorni, O. L. Lopera, and C. G. Windsor, "Estimation of relative permittivity of shallow soils by using the ground penetrating radar response from different

buried targets," *Progress In Electromagnetics Research Letters*, Vol. 2, 63–71, 2008.

9. Zhang, H., S. Y. Tan, and H. S. Tan, "An improved method for microwave nondestructive dielectric measurement of layered media," *Progress In Electromagnetics Research B*, Vol. 10, 145–161, 2008.
10. Rubinger, C. P. L. and L. C. Costa, "Building a resonant cavity for the measurement of microwave dielectric permittivity of high loss materials," *Microwave Opt. Tech. Lett.*, Vol. 49, 1687–1690, 2007.
11. Baker-Jarvis, J., E. J. Vanzura, and W. A. Kissick, "Improved technique for determining complex permittivity with the transmission/reflection method," *IEEE Trans. Microw. Theory Tech.*, Vol. 38, 1096–1103, 1990.
12. Chung, B.-K., "Dielectric constant measurement for thin material at microwave frequencies," *Progress In Electromagnetics Research,* PIER 75, 239–252, 2007.
13. Hasar, U. C., "Thickness-independent complex permittivity determination of partially filled thin dielectric materials into rectangular waveguides," *Progress In Electromagnetics Research*, PIER 93, 189–203, 2009.
14. Hasar, U. C., "A new microwave method based on transmission scattering parameter measurements for simultaneous broadband and stable permittivity and permeability determination," *Progress In Electromagnetics Research*, PIER 93, 161–176, 2009.
15. Hasar, U. C., "A microwave method for noniterative constitutive parameters determination of thin low-loss or lossy materials," *IEEE Trans. Microw. Theory Tech.*, Vol. 57, 1595–1601, Jun. 2009.
16. Hasar, U. C. and O. Simsek, "A calibration-independent microwave method for position-insensitive and nonsingular dielectric measurements of solid materials," *Journal of Phys. D: Appl. Phys.*, Vol. 42, 075403–075412, Mar. 2009.
17. Baker-Jarvis, J., M. D. Janezic, P. D. Domich, and R. G. Geyer, "Analysis of an open-ended coaxial probe with lift-off for nondestructive testing," *IEEE Trans. Microw. Theory Tech.*, Vol. 43, 711–718, 1994.
18. Stuchly, S. S. and M. A. Stuchly, "Coaxial line reflection method for measuring dielectric properties at radio and microwave frequencies, a review," *IEEE Trans. Instrum. Meas.*, Vol. 29, 1640–1648, 1999.

19. Teodoridis, V., T. Sphicopoulos, and F. E. Gardiol, "The reflection from an open-ended rectangular waveguide terminated by a layered dielectric medium," *IEEE Trans. Microw. Theory Tech.*, Vol. 33, 359–366, 1985.
20. Park, M. Y. and H. J. Eom, "Reflection coefficient of a flanged rectangular waveguide radiating into a dielectric slab," *Microw. Opt. Technol. Lett.*, Vol. 35, 401–404, 2002.
21. Bois, K. J., A. D. Benally, and R. Zoughi, "Multimode solution for the reflection properties of an open-ended rectangular waveguide radiating into a dielectric half-space: The forward and inverse problems," *IEEE Trans. Instrum. Meas.*, Vol. 48, 1131–1140, 1999.
22. Saleh, W. and N. Qaddoumi, "Potential of near-field microwave imaging in breast cancer detection utilizing tapered rectangular waveguide probes," *Computer and Electrical Engineering*, Vol. 35, 587–593, 2009.
23. Chang, C.-W., K.-M. Chen, and J. Qian, "Nondestructive determination of electromagnetic parameters of dielectric materials at X-band frequencies using a waveguide probe system," *IEEE Trans. Instrum. Meas.*, Vol. 46, 1084–1092, 1997.
24. Trabelsi, S. and S. O. Nelson, "Nondestructive sensing of physical properties of granular materials by microwave permittivity measurement," *IEEE Trans. Instrum. Meas.*, Vol. 55, 953–963, 2006.
25. Hasar, U. C., "Non-destructive testing of hardened cement specimens at microwave frequencies using a simple free-space method," *NDT & E Int.*, Vol. 42, 550–557, 2009.
26. Hasar, U. C., "A microcontroller-based microwave free-space measurement system for permittivity determination of lossy liquid materials," *Rev. Sci. Instrum.*, Vol. 80, 056103-1–056103-3, 2009.
27. Zoughi, R., *Microwave Non-destructive Testing and Evaluation,* Kluwer Academic Publishers, Dordrecht, The Netherlands, 2000.
28. Aydin, A. C., A. Arslan, and R. Gül, "Mesoscale simulation of cement based materials' time-dependent behavior," *Computational Materials Science*, Vol. 41, 20–26, 2007.
29. Bois, K. J., A. D. Benally, P. S. Nowak, and R. Zoughi, "Cure-state monitoring and water-to-cement ratio determination of fresh Portland cement-based materials using near-field microwave techniques," *IEEE Trans. Instrum. Meas.*, Vol. 47, 628–637, 1998.
30. Neville, A. M., *Properties of Concrete*, Longman Group, London, UK, 1996.

31. Malhotra, V. M. and N. J. Carino (eds.), *Handbook on Nondestructive Testing of Concrete*, CRC Press, Boca Raton, FL, 2004.
32. Cuinas, I. and M. G. Sanchez, "Building material characterization from complex transmittivity measurements at 5.8 GHz," *IEEE Trans. Antennas Propagat.*, Vol. 48, 1269–1271, 2000.
33. Balanis, C. A., *Advanced Engineering Electromagnetics*, John Wiley & Sons, New Jersey, NJ, 1989.
34. Oppenheim, A. V., A. S. Willsky, and S. Hamid, *Signals and Systems*, Prentice Hall, USA, 1997.
35. Hasar, U. C., "Two novel amplitude-only methods for complex permittivity determination of medium- and low-loss materials," *Meas. Sci. Techol.*, Vol. 19, 055706–055715, 2008.
36. Hasar, U. C., "Free-space non-destructive characterization of young mortar samples," *J. Mater. Civ. Eng.*, Vol. 19, 674–682, 2007.
37. Hasar, U. C., C. R. Westgate, and M. Ertugrul, "Permittivity determination of liquid materials using waveguide measurements for industrial applications," *IET Microw. Antennas Propag.*, Vol. 4, 10.1049/iet-map.2008.0197.
38. Hasar, U. C., C. R. Westgate, and M. Ertugrul, "Noniterative permittivity extraction of lossy liquid materials from reflection asymmetric amplitude-only microwave measurements," *IEEE Microw. Wireless Compon. Lett.*, Vol. 19, 419–421, 2009.
39. Bois, K. J., L. F. Handjojo, A. D. Benally, K. Mubarak, and R. Zoughi, "Dielectric plug-loaded two-port transmission line measurement technique for dielectric property characterization of granular and liquid material," *IEEE Trans. Instrum. Meas.*, Vol. 48, 1141–1148, 1999.
40. Chin, G. Y. and E. A. Mechtly, "Properties of materials," *Radio, Electronics, Computer, and Communications*, E. C. Jordan (ed.), 4-20–4-23, Howard W. Sams & Co., Indianapolis, IN, 1986.
41. Hasar, U. C. and C. R. Westgate, "A broadband and stable method for unique complex permittivity determination of low-loss materials," *IEEE Trans. Microw. Theory Tech.*, Vol. 57, 471–477, 2009.
42. Engen, G. F. and C. A. Hoer, "Thru-reflect-line: An improved technique for calibrating the dual six-port automatic network analyzer," *IEEE Microw. Theory and Tech.*, Vol. 27, 987–993, 1979.